Relationship between Solar Net Radiative Fluxes at the Top of the Atmosphere and at the Surface

JOHANNES SCHMETZ

European Space Agency, European Space Operations Centre, Darmstadt, Germany

(Manuscript received 20 February 1992, in final form 16 June 1992)

ABSTRACT

Previous work has discussed the existence of a linear relationship between the net solar radiative flux densities at the surface and at the top of the atmosphere (TOA) that can be exploited for inferring the net surface radiation directly from the satellite observed net radiation. In physical terms the net solar flux at the surface can be estimated from the difference between the satellite-inferred net flux at TOA and total solar absorption in the atmosphere.

This paper presents model calculations of the influence on solar absorption of water vapor, solar zenith angle, cloud-top altitude, and cloud optical thickness. The model results indicate a somewhat complex relation between the solar net fluxes at the surface and at the top of the atmosphere. It is pointed out that cloud altitude and optical depth have a large impact on solar atmospheric absorption; high clouds decrease solar absorption by the atmosphere whereas low clouds increase it. This difference between solar atmospheric absorption for low and high clouds increases with cloud optical depth. An intriguing result is that changes of total atmospheric absorption with cloud-top height are nearly completely compensated by corresponding changes in the net flux at the top of the atmosphere, thus leaving the surface solar net flux constant. Furthermore, this paper provides a very simple parameterization for estimating the clear-sky solar atmospheric absorption as a function of solar zenith angle and the vertically integrated water vapor content of the atmosphere.

1. Introduction

A simple linear relationship between the net solar radiation fluxes at the surface and at the top of the atmosphere (TOA) has been shown by Ramanathan (1986) and Cess and Vulis (1989). Cess et al. (1991) further examined this relationship and illustrated its usefulness for inferring the net solar flux at the surface (NET_{SFC}) from the net at the top of the atmosphere (NET_{TOA}) derived from satellite observations. Chou (1991) retrieved the surface net radiative flux from satellite radiance observations with a radiation model and demonstrated the significant influence of solar zenith angle on the relationship between NET_{TOA} and NET_{SFC}. Chertock et al. (1991) generated a seven-year climatology of NET_{SFC} from *Nimbus-7* planetary albedo observations and a theoretically modeled absorption by the atmosphere. The study by Pinker and Tarpley (1988) points out that solar scene brightness observed from a satellite may serve as a predictor for the total net surface radiation, which is due to the dominance of the solar contribution in the total net.

The existence of a linear relationship between the surface and TOA solar radiation fields is easily inferred from the solar radiative energy budget of an atmospheric column that can be written as:

$$NET_{TOA} = NET_{SFC} + S_{ABS}$$
$$= S{\downarrow}(1 - \alpha_{sfc}) + s_{abs} S_0 \cos\theta_0 \qquad (1)$$

where NET_{TOA} and NET_{SFC} are the solar net flux at the top of the atmosphere and at the surface, S_{ABS} is the radiative energy absorbed in the atmosphere, $S{\downarrow}$ is the solar surface irradiance or insolation, α_{sfc} the surface albedo, s_{abs} the fractional solar absorption, S_0 the solar constant, and θ_0 the solar zenith angle.

Equation (1) is valid on a scale where horizontal radiative transport is negligible, that is, for a scale larger than convective clouds, for which the leaking of photons through cloud sides is important (e.g., McKee and Cox 1974). Equation (1) shows that NET_{SFC} can be retrieved from NET_{TOA} with an adequate estimate of S_{ABS}.

Equation (1) implies that the surface radiation field is linearly related to the satellite-observed solar radiation if solar absorption does not impose a strong nonlinearity. This generally is the case for two reasons. First, s_{abs} has a relatively small range of variability of about 15%–30% of the incoming solar flux at TOA over all realistic atmospheric conditions (cf. Figs. 1 and 4). That is, the natural variability of S_{ABS} is considerably smaller than the variability of both NET_{TOA}

Corresponding author address: Dr. Johannes Schmetz, European Space Agency, European Space Operations Centre, Robert Bosch-Str. 5, Darmstadt, W-6100, Germany.

and NET_{SFC}. Second, it appears that S_{ABS} varies linearly with cloud albedo if other atmospheric conditions, in particular cloud-top height, are held fixed. This has been shown previously by multispectral Monte Carlo calculations (Schmetz 1984, 1989) and with aircraft measurements (Rawlins 1989).

Atmospheric absorption is affected by solar zenith angle θ_0, water vapor, ozone, aerosol, clouds, and to a lesser extent by CO_2, O_2, and other minor constituents. Some sensitivity studies on solar absorption or transmission have been conducted previously (e.g., Davies et al. 1984; Chou 1989; Schmetz 1989).

The purpose of this paper is to investigate total solar absorption by the earth's atmosphere with respect to methods for transferring satellite solar net flux measurements to the surface. First, the influence of both solar zenith angle and the vertically integrated water vapor, hereafter called total-column water vapor or precipitable water, on fractional solar absorption s_{abs} is discussed. A very simple parameterization for the dependence of s_{abs} on solar zenith and precipitable water is developed. The parameterization is derived from a regression analysis on spectral radiative transfer calculations. It provides an easy means for estimating S_{ABS} and for inferring NET_{SFC} from NET_{TOA} in clear sky. Second, the effect of clouds on solar atmospheric absorption is discussed with respect to the retrieval of NET_{SFC} from satellite observations of NET_{TOA}. The main point here is to illustrate the relevant issues. Specific applications will necessitate additional quantitative analyses.

The paper proceeds as follows. The next section describes the radiative transfer model and its performance in a recent intercomparison of shortwave radiation codes. In section 3 the dependence of s_{abs} on θ_0 and total-column water vapor u is parameterized. Section 4 briefly addresses the influence of aerosol, surface albedo, and ozone on solar atmospheric absorption. Section 5 investigates the importance of cloud-top height and optical depth.

2. Radiation model

The multispectral radiation model (Schmetz 1984) uses a delta-two-stream formulation and has 37 spectral bands resolving the spectrum between 0.2 and 4 μm and considers:

TABLE 1. Aerosol profile used in this study following World Climate Research Programme (1986): g denotes the asymmetry factor, ω is the single scattering albedo, and δ is the optical depth, all referring to a wavelength of 0.55 μm.

Altitude interval (km)	Aerosol type	g	ω	δ
0–2	maritime	0.744	0.988	0.181
2–10	continental	0.637	0.891	0.061
10–50	stratospheric	0.726	1.000	0.008

TABLE 2. Total atmospheric absorption for different atmospheric conditions. The case numbers in the first column refer to ICRCCM (Intercomparison of Radiation Codes Used in Climate Models; Fouquart et al. 1991). Comparison is made between the median value of models participating in ICRCCM (from Fouquart et al. 1991) and the model used in this study. Abbreviations MLS, SAW, and TRO denote standard atmospheres characteristic of midlatitude summer, subarctic winter, and a tropical atmosphere after McClatchey et al. (1972). Details on the aerosol profiles are given in Fouquart et al. (1991).

Case (*)	Model atmosphere	Solar zenith angle	S_{ABS}/ICRCCM (W m^{-2})	S_{ABS}/this model (W m^{-2})
31	MLS	30°	206.2	202.8
33	MLS	75°	83.8	78.9
35	TRO	30°	215.1	209.3
37	TRO	75°	84.0	79.3
39	SAW	30°	150.6	157.1
41	SAW	75°	66.6	66.7
43	MLS: Cloud top 13 km	30°	203.4	198.4
45	MLS: Cloud top 2 km	30°	226.7	225.8
50	MLS: Aerosol maritime I	30°	214.7	208.6
54	MLS: Aerosol maritime II	30°	601.2	593.3

(i) Molecular Rayleigh scattering.

(ii) Gaseous absorption by water vapor, ozone, carbon dioxide, and oxygen, which is computed from exponential-sum fits to transmittances (Raschke and Stucke 1973; Wiscombe and Evans 1977). Water vapor transmission fits are based on LOWTRAN-5 (Kneizys et al. 1980), while other gaseous absorbers are treated as in Kerschgens et al. (1976).

(iii) Absorption and scattering by aerosol. Specifically, this study assumes a profile combined of three different aerosol types as specified by the World Climate Research Programme (1986), the details of which are summarized in Table 1. It is noteworthy that the maritime and continental aerosol in Table 1 correspond to the MAR-I and MAR-II aerosol types as used by Fouquart et al. (1991).

(iv) Absorption and scattering by cloud droplets. This study assumes a size distribution with an effective radius of 5.35 μm following Stephens (1979; his Sc I cloud). The cloud is specified in the radiation model in terms of spectral extinction and absorption coefficients and spectral asymmetry parameters. The spectral variability of the cloud parameters is accounted for by ten spectral intervals, seven of which are in the water vapor absorption range between 0.71 and 4 μm.

(v) A spectrally flat surface albedo $\alpha_{sfc} = 0.2$; except for the sensitivity tests in section 4.

The model has been tested within the International Comparison of Radiation Codes for Climate Models (ICRCCM; Fouquart et al. 1991). Table 2 provides a comparison of total atmospheric absorption S_{ABS} be-

tween the median value of all radiation models that participated in ICRCCM and our radiation model. The median values are taken from the relevant tables in Fouquart et al. (1991). Generally the agreement in Table 2 is within 5 W m^{-2}; however, there is a tendency for our model to underestimate S_{ABS} at high column-water vapor u in moist atmospheres (e.g., tropical and midlatitude summer: TRO and MLS, respectively) and vice versa at low u (subarctic winter: SAW). The water vapor absorption of our scheme is based on exponential-sum fits to LOWTRAN-5; as shown by Fouquart et al. (1991), the LOWTRAN-rooted models all exhibit this tendency. It is noted that the bias is slightly more pronounced in comparison to line-by-line calculations for a purely absorbing water vapor atmosphere (cf. Table 6 in Fouquart et al. 1991) and reaches about 7% (about 12 W m^{-2}) for TRO at $\theta_0 = 30°$. Certainly line-by-line models constitute the accepted standard for other radiation models (e.g., Ramaswamy and Freidenreich 1991); however, it is, for the time being, not clear how accurate line-by-line results are until they have been validated through high-resolution spectral measurements (Fouquart et al. 1991).

3. Atmospheric absorption as function of solar zenith and column water vapor

The above radiation model has been used to compute the atmospheric absorption S_{ABS} for different model atmospheres as a function of solar zenith angle. The importance of solar zenith angle for the relationship between fluxes at the surface and at the satellite level has been emphasized recently by Chou (1991). It is interesting that the relationship between the fractional absorption s_{abs} and solar zenith can be accurately fitted with:

$$s_{abs}(\theta_0) = \frac{S_{ABS}}{S_0 \cos\theta_0} = 1 - ab^m \qquad (2)$$

where a and b are regression coefficients and $m = 1/\cos\theta_0$ is the relative optical air mass of the plane-parallel atmosphere. Regression fits analogous to Eq. (2) have been used before in order to parameterize clear-sky solar transmission (Schmetz and Raschke 1978). Figure 1 shows radiative transfer results (crosses) for three model atmospheres after McClatchey (1972), namely, tropical (TRO), midlatitude summer (MLS), and midlatitude winter (MLW). Solid lines in Fig. 1 depict fits to the model results based on Eq. (2) with regression coefficients as provided in Table 3. For all three atmospheres the linear correlation coefficient of the fit is higher than 0.999 and rms differences between model results and fit are between 0.003 for MLW and 0.007 for TRO.

The radiative transfer model assumes a plane-parallel atmosphere; therefore, the optical path becomes too large for large solar zenith angles. Consequently, only radiative transfer results between $\theta_0 = 0°$ and 75° have been used in the regression, yet Eq. (2) can be extended to a spherical shell atmosphere using an appropriate formula for the relative air mass (e.g., Kasten and Young 1989).

The differences in fractional solar absorption for the three model atmospheres shown in Fig. 1 are mainly due to different column-water vapor. Therefore, a useful extension to Eq. (2) is to include the dependence on column-water vapor. Table 3 reveals that the coefficient b varies little for the three different atmospheres. This suggests that a variable column-water vapor u can be accounted for by taking the coefficient a as a function of u. A Taylor series expansion of Eq. (2) yields:

$$s_{abs}(u) = s_{abs}(u_0) + s'_{abs}(u_0)(u - u_0) + \frac{s''_{abs}(u_0)}{2}(u - u_0)^2 + \cdots \approx 1 - ab^m - b^m(u - u_0)\left.\frac{\partial a}{\partial u}\right|_{u_0} - b^m(u - u_0)^2\left.\frac{\partial^2 a}{2\partial u^2}\right|_{u_0} \qquad (3)$$

where $s_{abs}(u_0)$ is the fractional atmospheric absorption at the reference column-water vapor u_0, and a and b are the corresponding coefficients, while prime and double prime denote first and second derivative, respectively.

Taking a MLS atmosphere with $u = 2.9$ cm precipitable water and standard profiles for aerosol and other gaseous constituents as reference, the parameterization for the fractional solar absorption s_{abs} as a function of solar zenith angle and precipitable water reads:

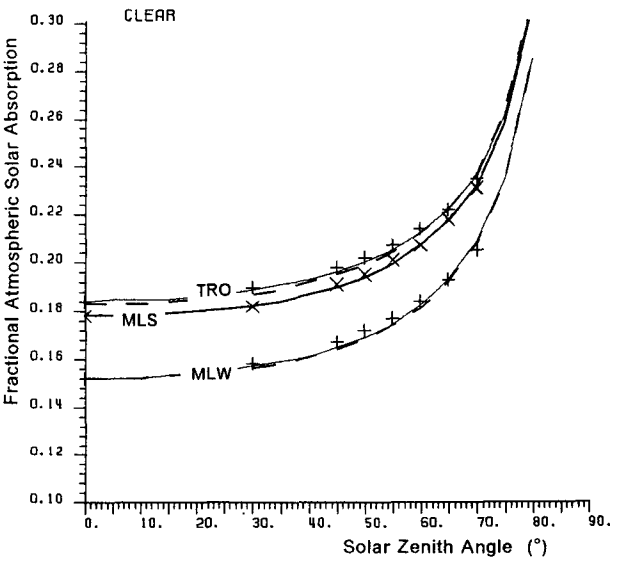

FIG. 1. Fractional atmospheric solar absorption as a function of solar zenith angle for three standard model atmospheres (TRO: tropical, MLS: midlatitude summer, MLW: midlatitude winter). Crosses depict model results, solid lines are the specific fits based on Eq. (2) using the coefficients in Table 3, while the dashed lines correspond to the parameterization in Eq. (4).

TABLE 3. Regression coefficients for Eq. (2) for different standard atmospheres.

Model atmosphere	a	b
Tropical (TRO)	0.844	0.966
Midlatitude summer (MLS)	0.852	0.965
Midlatitude winter (MLW)	0.879	0.965

$$s_{abs}(\theta_0, u) = 1 - ab^m - b^m(u - u_0)[a_1 + a_2(u - u_0)] \quad (4)$$

with $u_0 = 2.9$ cm, a and b as given in Table 3 for the MLS atmosphere, $a_1 = -0.0077$, and $a_2 = 0.0025$. Both a_1 and a_2 have been derived from an analysis of the dependence of the coefficient a on column-water vapor, where a_2 has been somewhat increased in order to improve the fit.

Equation (4) provides a very simple means for estimating the total atmospheric absorption as a function of solar zenith angle and precipitable water. Aerosol and ozone profiles underlying Eq. (4) correspond to the standard MLS atmosphere with a surface albedo of 0.2. The potential effects of those parameters are briefly discussed in section 4.

It should be mentioned that there are several simple parameterizations for computing solar absorption by water vapor, ozone, oxygen, and carbon dioxide (e.g., Chou 1986; Lacis and Hansen 1974; Kiehl et al. 1985; Chou 1990). It is not claimed that the present very simple fit performs any better. However, the present parameterization appears attractive since detailed radiation calculation can be fitted easily with a linear regression by taking the logarithm of Eq. (2). As a useful application of this simple parameterizations, see a real-time retrieval of surface solar net fluxes from TOA net fluxes. Highly accurate clear-sky radiation calculations for a variety of atmospheric conditions could be conducted off-line and then be fitted with Eq. (2) or (4). The real-time retrieval of clear-sky surface solar net fluxes then would not require time consuming radiation computations but only the application of the specific fit appropriate to the meteorological conditions. The fit still provides flexibility to consider solar zenith angle and precipitable water.

The performance of Eq. (4) is also shown in Fig. 1. The dashed lines pertain to the parameterization [Eq. (4)] using the precipitable water $u = 0.85$ cm and $u = 4.1$ cm for the MLW and TRO atmosphere, respectively. It is to be seen that Eq. (4) virtually coincides with the specific fits to TRO and MLW, although the parameterization does not consider the actual ozone absorption path length. The rms differences between model results (crosses) and parameterization are less than 0.007 for the fractional absorption.

Figures 2 and 3 will address the issue of a single linear relationship for transferring satellite net flux measurements to the surface without considering solar zenith angle. Figure 2 shows the relationship between the net fluxes at the surface and at the top of the atmosphere for clear sky as computed with the radiation model. Calculations encompass eight solar zenith angles (0°, 30°, 45°, 50°, 55°, 60°, 65°, and 70°) and seven different atmospheres, that is, a total of 56 data pairs. The atmospheres comprise MLW, TRO, MLS, and four modifications of MLS where the column-water vapor has been modified such that $u = 5.8$, 3.48, 2.32, and 0.58, respectively. We observe a high linear correlation, although the data cover a zenith angle range between 0° and 70°, a fact that has already been pointed out by Cess et al. (1991).

Figure 2 would suggest a retrieval of NET_{SFC} from NET_{TOA} for clear sky via a single empirical linear regression without the need to consider solar zenith angle. This has been done in Fig. 3a where NET_{SFC} has been computed from a linear regression (first principal component) to the data in Fig. 2. The comparison is made in Fig. 3a between the estimate and exact model results. A fairly close agreement is observed with an rms difference of 15.8 W m^{-2} or 3.1% of the average.

Figure 3b is similar to Fig. 3a except that the estimated NET_{SFC} has been computed from NET_{TOA} minus S_{ABS} as calculated from Eq. (4); that is, both zenith angle and column-water vapor are explicitly considered. In comparison to Fig. 3a the rms difference has been reduced to 7.1 W m^{-2} (1.4%), which demonstrates that a physical method for inferring NET_{SFC} from NET_{TOA} is superior to the purely statistical approach. Admittedly, there are factors that compromise the use of Eq. (4), especially the variable atmospheric

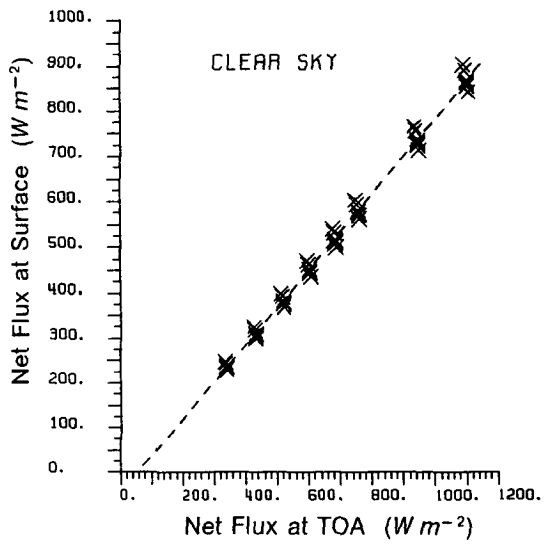

FIG. 2. Net solar radiation at the surface (NET_{SFC}) versus net solar at the top of the atmosphere (NET_{TOA}) for 8 solar zenith angles and several clear-sky atmospheres (for details see text). The linear regression equation reads:

$$NET_{SFC} = 0.828NET_{TOA} - 47.4 \text{ [W m}^{-2}\text{]}.$$

The linear correlation coefficient is 0.99.

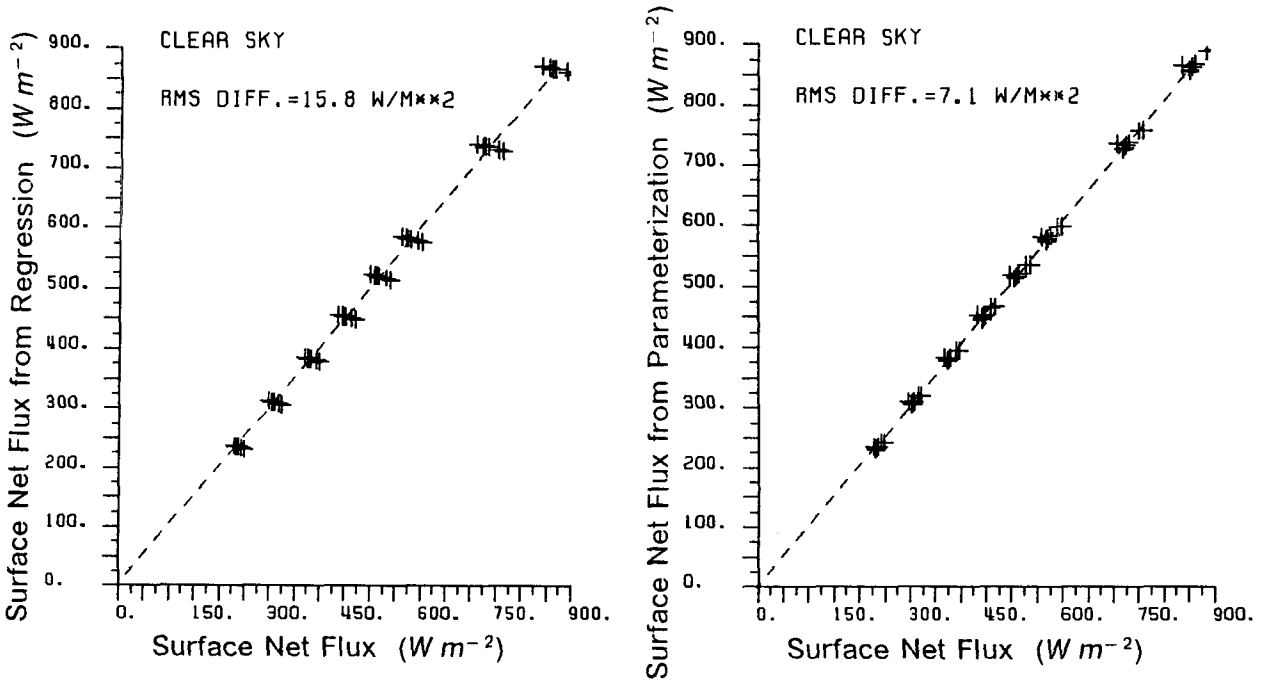

FIG. 3. (a) NET_{SFC} retrieved from the linear regression between NET_{TOA} and NET_{SFC} in Fig. 2 versus the exact results. Atmospheric conditions are clear sky as in Fig. 2. (b) As in (3a) except that NET_{SFC} has been estimated from NET_{TOA} minus solar atmospheric absorption S_{ABS} as computed via Eq. (4).

loading with absorbing aerosol; however, those factors also detract from the usefulness of empirical slope-offset relationships that are derived from a particular dataset and, therefore, are not generally applicable in other climatological regions. A problem with Eq. (4) may arise from the bias inherent in the radiative transfer calculations; as mentioned above, this can be alleviated through future model validation by high-resolution spectral measurements.

4. Influence of aerosol, surface albedo, and ozone

In the brief discussion of this section the sensitivity of the clear-sky solar absorption to aerosol, surface albedo, and ozone is investigated. Model calculations have been performed for various modifications of the MLS standard atmosphere, with $\alpha_{sfc} = 0.2$ and an aerosol optical depth of 0.25, as assumed in the previous sections. A summary is given in Table 4, where also the fit parameters a and b for Eq. (2) are provided.

Aerosol. The fractional absorption for the standard MLS atmosphere with an aerosol optical depth of 0.25 and $\theta_0 = 0°$ is $s_{abs} = 0.178$. A simple doubling of the aerosol optical depth while keeping the aerosol types constant (see Table 1) increases s_{abs} to 0.19. The increase is of s_{abs} is mainly due to the increase of the continental aerosol in the layer between 2 and 10 km. If the doubling of aerosol optical depth is combined with a change of the aerosol type in the lowest 2 km from maritime to continental, s_{abs} increases to as much as 0.227. At a solar zenith angle of 0° a difference of 3% in fractional solar absorption amounts to about 40 W m^{-2}, which illustrates that absorbing aerosols can have a large impact on retrievals of NET_{SFC}. Additional conservative scatterers only have a little effect through the increased absorption due to increased photon pathlength (Cess and Vulis 1989).

One can conclude that ancillary information on aerosol optical depth and aerosol type would greatly enhance the accuracy of satellite-based retrievals of solar net fluxes at the surface. Aerosol optical depth over the oceans is available as a product from polar orbiting satellites (Rao et al. 1989) and aerosol type could also be estimated from climatology (d'Almeida et al. 1991).

TABLE 4. Regression coefficients for Eq. (2) for variations of the standard midlatitude summer atmosphere (MLS). The standard MLS calculations (first row) assume an aerosol profile with $\delta_{aer} = 0.25$, the aerosol characteristics of Table 1 and a surface albedo $\alpha_{sfc} = 0.2$.

Model atmosphere	a	b
MLS	0.852	0.965
MLS: $\delta_{aer} = 0.5$	0.843	0.961
MLS: $\delta_{aer} = 0.5$; 0–2 km continental aerosol	0.820	0.943
MLS: no aerosol	0.857	0.971
MLS: $\alpha_{sfc} = 0$	0.866	0.962
MLS: $\alpha_{sfc} = 0.6$	0.822	0.970
MLS: $O_3 \times 0.7$	0.854	0.967
MLS: $O_3 \times 1.3$	0.850	0.962

Surface albedo. The atmospheric absorption increases with surface albedo due to increased multiple reflection between surface and atmosphere. Table 4 contains, in addition to the standard $\alpha_{sfc} = 0.2$, results for $\alpha_{sfc} = 0$ and 0.6, respectively. One can calculate the sensitivity of s_{abs} to surface albedo for $\theta_0 = 0°$ and obtains:

$$\left.\frac{\Delta s_{abs}}{\Delta \alpha_{sfc}}\right|_{\alpha_{sfc}\approx 0.2} \approx 0.06. \quad (6)$$

That is a modest sensitivity; for instance, a variation of 0.1 in α_{sfc} induces a systematic error of about 0.006 in s_{abs}.

This effect can easily be considered in Eq. (2) by a linear interpolation for both coefficients a and b as a function of α_{sfc}. Specifically, a linearly decreases with increasing α_{sfc}:

$$a(\alpha_{sfc}) = 0.866 - 0.0733\ \alpha_{sfc} \quad (7)$$

whereas b increases with increasing α_{sfc}:

$$b(\alpha_{sfc}) = 0.962 + 0.0133\alpha_{sfc}. \quad (8)$$

It is also noted that the sensitivity of s_{abs} to α_{sfc} looks different from Eq. (6) for surfaces with spectrally varying reflectances. It is beyond the scope of the present work to elaborate this effect.

Ozone. In the test calculations the ozone profile has been shifted by multiplying the ozone mixing ratio with 0.7 and 1.3, corresponding to ozone pathlengths of 0.217 cm STP and 0.403 cm STP, respectively. The change in s_{abs} is from 0.178 to 0.174 and 0.182, respectively. Thus, the linearized sensitivity of s_{abs} to O_3 variations in a standard MLS atmosphere is fairly small with about

$$\left.\frac{\Delta s_{abs}}{\Delta O_3}\right|_{O_3=0.31\ \text{cm-STP}} \approx 0.043\ (\text{cm} - \text{STP})^{-1} \quad (9)$$

5. Influence of clouds

In cloudy atmospheres the estimation of s_{abs} appears to be complicated by a dependence on cloud-top height (Chou 1989; Schmetz 1991). Figures 4a and 4b illustrate the point by results from the radiation model for a MLS standard atmosphere and ten solar zenith angles. The dashed line shows the clear-sky absorption as a function of zenith angle that has been parameterized in the previous section. Solid lines depict results for the same cloud embedded at altitudes of 1, 2, 4, 7, 10, and 13 km, respectively. The cloud consists of water droplets with an effective radius of 5.35 μm (Stephens 1979), is 1 km thick and has an optical depth of $\delta_{0.55\,\mu m} = 57$ (Fig. 4a) and 5.7 (Fig. 4b), respectively. We observe the following characteristics of fractional solar atmospheric absorption:

- Low clouds increase fractional atmospheric solar absorption s_{abs} in comparison to clear sky. The effect

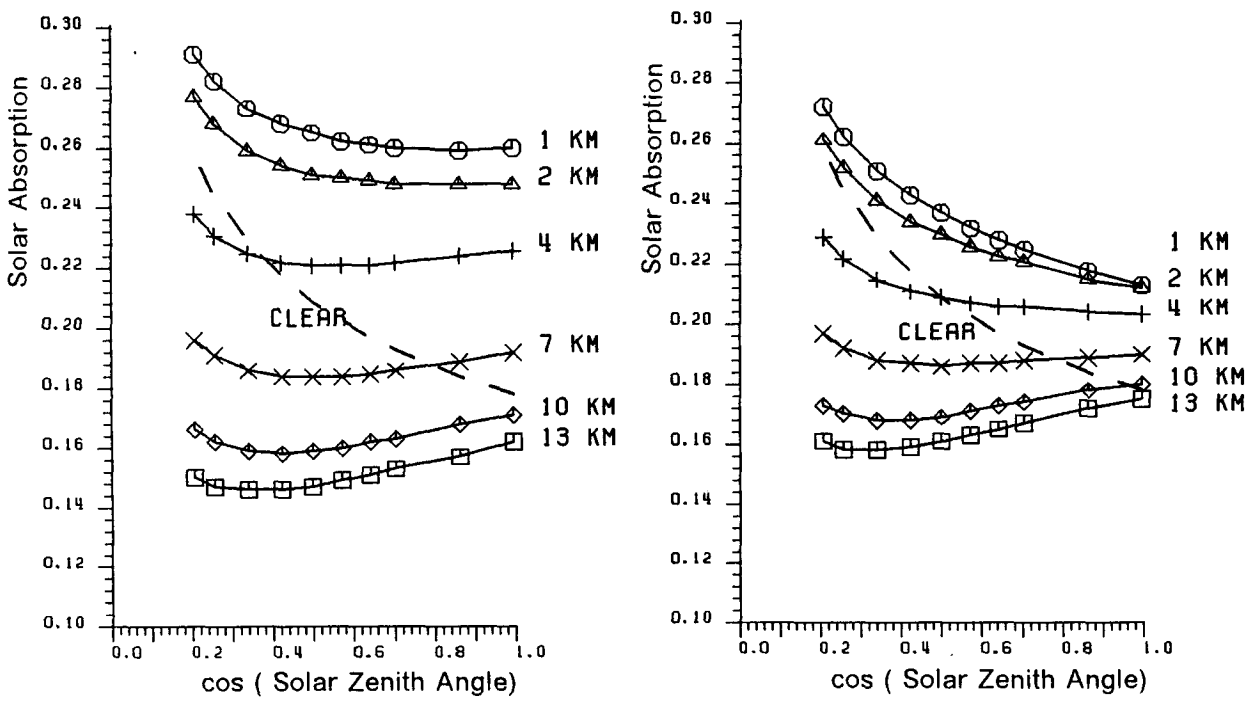

FIG. 4. (a) Fractional atmospheric solar absorption versus cosine of the solar zenith angle for a clear MLS atmosphere (dashed) and cloud tops at different altitudes. Cloud optical depth is $\delta_{0.55\,\mu m} = 57$ and the geometric thickness is 1 km. (b) As in (a) except for $\delta_{0.55\mu m} = 5.7$.

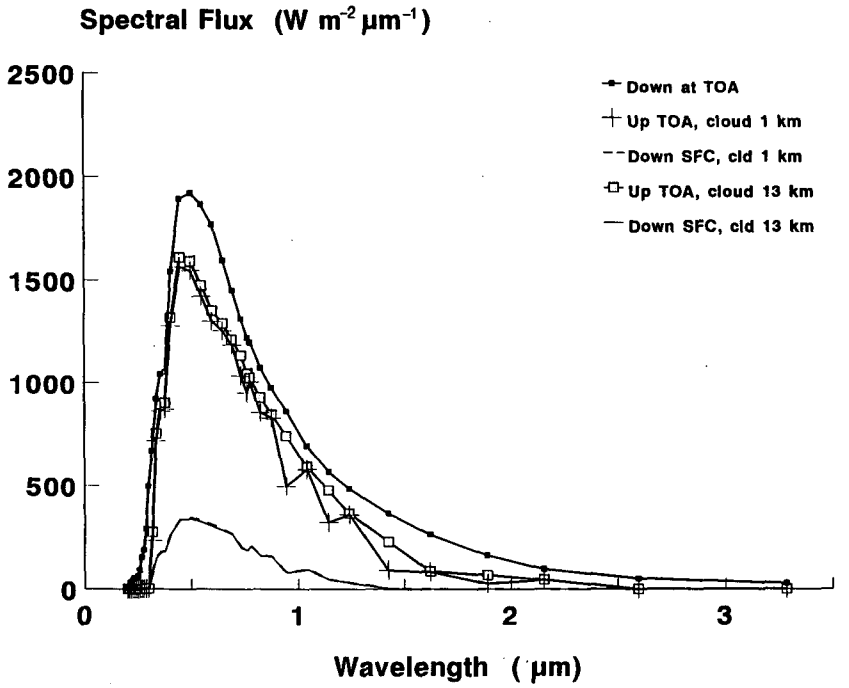

FIG. 5a. Different solar spectral fluxes (W m^{-2} μm^{-1}) versus wavelength for two cloud-top altitudes (1 km and 13 km, respectively). Cloud optical thickness at a wavelength of 0.55 μm is $\delta_{cld} = 57$ Solar zenith angle is $\theta_0 = 0°$ and a midlatitude summer atmosphere is assumed. Solid squares: spectral downward flux at the top of the atmosphere. Open squares: spectral upward flux at the top of the atmosphere for a cloud at 13 km. Crosses: spectral upward flux at the top of the atmosphere for a cloud at 1 km. Solid line: spectral downward flux at the surface for cloud at 13 km. Dashed line: spectral downward flux at the surface for cloud at 1 km.

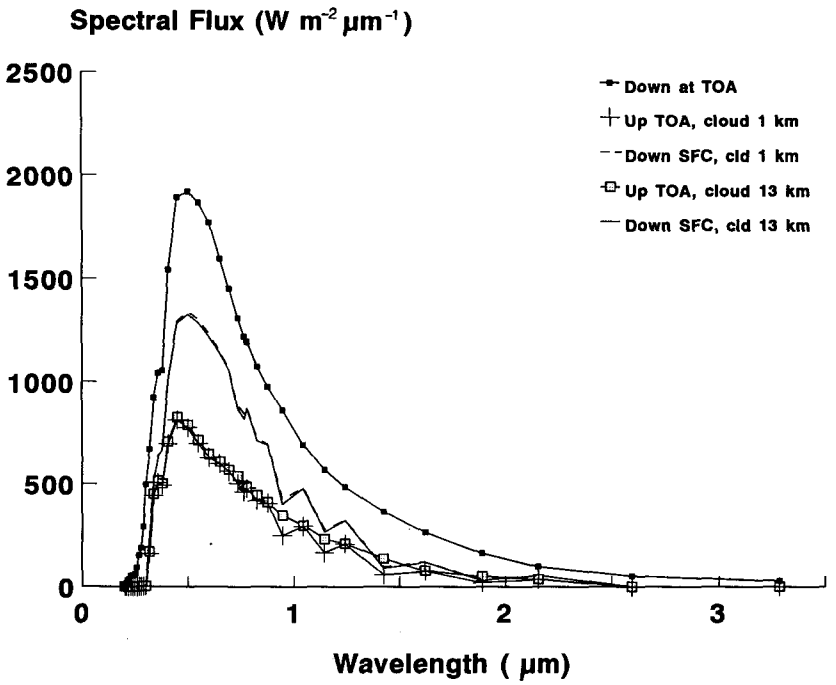

FIG. 5b. As Fig. 5a except for an optical thickness of $\delta_{cld} = 5.7$.

is strongest at small solar zenith angles. High clouds reduce solar absorption especially at large solar zenith angles.

- The decrease in s_{abs} for high clouds is mainly due to decreased water vapor absorption in the near-infrared and to a lesser extent due to a decrease of ozone absorption in the Chappuis band and O_2 and CO_2 absorption, respectively. Figures 5a and 5b illustrate this by showing the spectral fluxes for clouds at 1-km and 13-km altitude embedded in an MLS atmosphere and a solar zenith angle of $\theta_0 = 0°$. The enhanced water vapor absorption in the near-infrared for a low cloud is evident in Figs. 5a and 5b as significant drops in the curve for the reflected spectral flux at the top of the atmosphere.
- The solar zenith angle dependence of s_{abs} is quite different than for clear sky. For a given cloud altitude the range of the dependence of s_{abs} on θ_0 is reduced. This is consistent with Davies et al. (1984), who found little change in total solar absorption with solar zenith for a low cloud at 2 km and solar zenith angles up to 60°.
- Variation of total solar absorption s_{abs} with cloud altitude is more important than the solar zenith angle dependence. The effect is more pronounced for optically thick clouds than for optically thin clouds.

The preceding results lead to the conclusion that the estimation of s_{abs} in cloudy cases necessitates the consideration of cloud-top height and optical depth. Previous work has shown that other factors such as cloud phase and droplet size (e.g., Wiscombe et al. 1984; Newiger and Baehnke 1981) and aerosol inside the cloud (e.g., Grassl 1975) are important, yet those topics are not addressed in this paper.

The complex dependence of s_{abs} on both cloud height and optical depth does not allow to fit the model results with a simple physical parameter equation as it is possible for clear sky. When s_{abs} estimates are needed in real time or for large data volumes, for instance, for deriving a surface net radiation climatology, it is proposed to use a radiative transfer code or to construct a retrieval algorithm based on precomputed lookup tables that would alleviate the problem of computing time. A prerequisite for such an algorithm is a preprocessing of satellite data that includes an adequate scene identification.

Figure 6 examines the influence of clouds on a linear slope–offset relationship between NET_{SFC} and NET_{TOA}. Three parameters have been varied in the model calculations of Fig. 6:

(i) cloud optical depth δ_{cld} (clear tropical atmosphere, $\delta_{cld} = 0.57, 5.7, 57$, respectively);
(ii) solar zenith angle (30° and 60°);
(iii) cloud-top height (2 km and 13 km).

We observe that varying the optical depth provides a linear relationship between NET_{SFC} and NET_{TOA}.

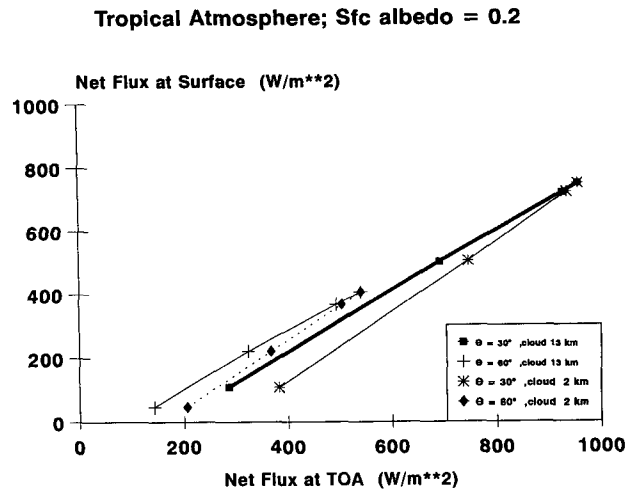

FIG. 6. NET_{SFC} as a function of NET_{TOA} for different solar zenith angles and cloud tops (2 km and 13 km). Straight lines correspond to variations in cloud optical depths ($\delta = 0, 0.57, 5.7, 57$). Note that linear relationships change with solar zenith and especially with cloud-top height. The model atmosphere is characteristic of the tropics. Regression lines read:

$NET_{SFC} = 0.953NET_{TOA} - 163$: for $\theta_0 = 30°$ and cloud top at 13 km

$NET_{SFC} = 1.112NET_{TOA} - 320$: for $\theta_0 = 30°$ and cloud top at 2 km

$NET_{SFC} = 0.901NET_{TOA} - 78$: for $\theta_0 = 60°$ and cloud top at 13 km

$NET_{SFC} = 1.072NET_{TOA} - 173$: for $\theta_0 = 60°$ and cloud top at 2 km.

(NET_{SFC} and NET_{TOA} are in W m^{-2}.)

This is understood from the fact that the system (and planetary) albedo varies linearly with atmospheric absorption as has been shown previously by theoretical (Schmetz 1984, 1989) and experimental (Rawlins 1989) work. However, a particular slope-offset relationship holds true only for a particular solar zenith, as already emphasized by Chou (1991), and a particular cloud-top altitude.

Figure 6 reveals that the difference in atmospheric absorption between a thick cloud at 2-km and 13-km altitude is as large as 100 W m^{-2} for $\theta_0 = 30°$. It is also intriguing that for low-level clouds, which increase atmospheric absorption in comparison to clear sky, the slope of the linear relationship is greater than one (see caption of Fig. 6). High clouds have a solar cooling effect on the atmospheric column that corresponds to a slope of less than one. Supporting evidence that low clouds enhance total solar absorption whereas high clouds cause less absorption than clear sky is given by Cess et al. (1993).

Further convincing evidence of the importance of cloud-top height on the relationship between NET_{SFC}

and NET_{TOA} is shown in Fig. 7. The net fluxes NET_{SFC} and NET_{TOA} are plotted as a function of cloud-top height for two solar zenith angles (0° and 60°), two different optical depths, and two surface albedos, as indicated in the panel insertions of Fig. 7. Remarkably, the surface net flux NET_{SFC} remains virtually constant, whereas NET_{TOA} decreases with increasing cloud height. The surface net flux decreases only from 616 W m^{-2} for the thin cloud at 1 km to 604 W m^{-2} for a cloud at 13 km assuming $\alpha_{sfc} = 0.2$. This change is quite small compared to the corresponding change in NET_{TOA} from 906 W m^{-2} to 842 W m^{-2}. This result is consistent with Chou (1989), who has shown (his Fig. 6) the same feature for the near-infrared solar flux. Thus, changes in atmospheric absorption with cloud-top height are nearly completely reflected in changes in NET_{TOA}. The reason is that solar transmittance through the cloud is very similar in the solar infrared for different cloud heights, whereas cloud and planetary albedo is significantly higher in the solar absorption bands for the high-level cloud (see Figs. 5a and 5b).

It is noted that the above finding also has implications on retrievals of solar surface insolation from satellite radiance observations (for an overview, see references in Schmetz 1989), because it demonstrates that surface insolation is quite insensitive to cloud-top height, yet the satellite-observed broadband radiation field is not. An important conclusion is that simple regression retrievals of surface insolation for global application will work well only if the satellite radiance observations are outside the regions of solar absorption, because only there the relationship between radiation fields at the top of the atmosphere and at the surface is little affected by atmospheric absorption. Since most solar channels aboard operational meteorological satellites are outside the regions of water vapor absorption

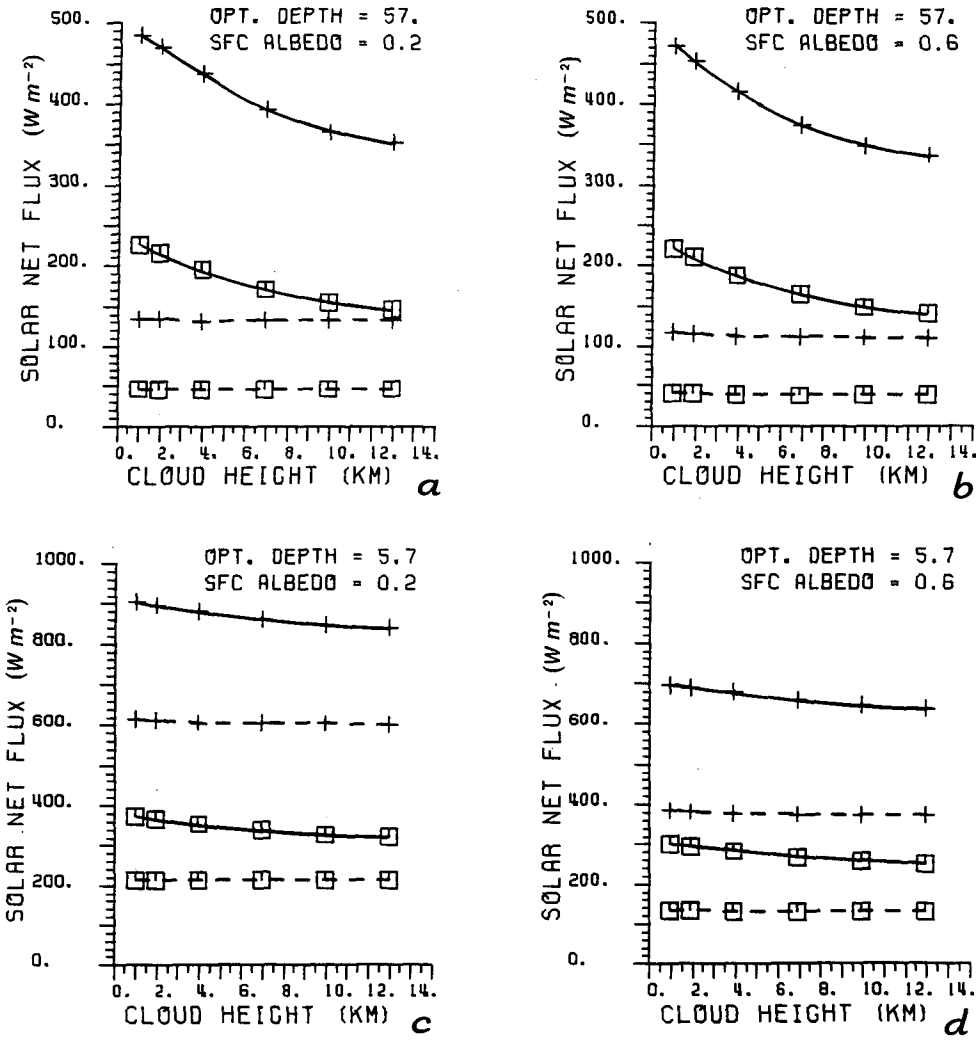

FIG. 7. NET_{SFC} (dashed) and NET_{TOA} (solid) versus cloud-top height for two solar zenith angles $\theta_0 = 0°$ (crosses) and $\theta_0 = 60°$ (squares). The four panels show results for two cloud optical thicknesses ($\delta_{cld} = 57$ and $\delta_{cld} = 5.7$) and two surface albedoes ($\alpha_{sfc} = 0.2$ and $\alpha_{sfc} = 0.6$) as indicated in panels (a) through (d).

(Meteosat being an exception), this may also explain why satellite retrievals of surface insolation work so well even under cloudy conditions. It appears worthwhile to further examine this point in a study with measured data and with a model of higher spectral resolution.

A short remark is due concerning the influence of surface albedo on solar atmospheric absorption in cloudy sky. Generally speaking, a higher surface albedo enhances multiple reflection between surface and atmosphere, which in turn increases the photon pathlength and hence atmospheric absorption. Model calculations show that the effect is marginal for optically thick clouds since little radiation penetrates the cloud and reaches the surface; for instance, for a cloud with $\delta_{cld} = 57$ embedded between 1 and 2 km and $\theta_0 = 0°$, an increase of α_{sfc} from 0.2 to 0.6 only changes s_{abs} from 0.248 to 0.251. For a thin cloud with $\delta_{cld} = 5.7$ the corresponding increase in s_{abs} is quite significant from 0.212 to 0.230.

6. Concluding remarks

In climate and energy budget studies the net surface solar flux generally is the quantity of interest. Consequently, it has been suggested (Cess et al. 1991; Chou 1991) that NET_{SFC} be retrieved directly from the satellite observations without diverting to separate estimates of surface solar irradiance and surface albedo. The principle of solar radiative energy conservation within an atmospheric column [see Eq. (1)] directly suggests a simple retrieval algorithm that requires only an estimate of atmospheric solar absorption as correlative data to the satellite inferred net flux at the top of the atmosphere.

In this paper the dependence of total atmospheric absorption on gaseous absorbers, aerosol, and especially clouds is investigated. In particular, it has been demonstrated that accurate estimation of solar atmospheric absorption also requires cloud-top height and optical depth to be considered. In comparison to clear-sky absorption, low clouds increase total atmospheric solar absorption S_{ABS} where the effect is most pronounced at low solar zenith angles. High clouds have the opposite effect and decrease S_{ABS}. For an optically thick cloud ($\delta = 57$) at 2 km and 13 km, respectively, the difference in S_{ABS} can be as large as 100 W m^{-2}.

It should be mentioned that the modulating effect of cloud altitude on spectral solar absorption in the atmosphere is known and is being used for inferring cloud-top altitude from spectral satellite measurements (Fischer and Grassl 1991).

The radiation model computations show very little influence of cloud-top height on the surface downward irradiance. That is, the increase (decrease) of solar atmospheric absorption induced by cloud-top height changes is virtually balanced by a decrease (increase) in planetary albedo if nothing but cloud-top height is changed. This finding also points at limitations inherent in empirical regression algorithms for inferring surface insolation from spectrally integrated satellite radiation observations, since the relationship between broadband solar radiation fields at the surface and at the top of the atmosphere is not unique.

As a practical approach to an inference scheme for NET_{SFC} from satellites, we suggest lookup tables for various cloudy conditions and surface albedos that were precomputed with a radiation code. The application of the lookup retrieval necessitates a scene identification that specifies cloud conditions.

A simple parameterization has been developed for the dependence of fractional solar absorption on solar zenith angle and precipitable water. The parameterizations ought to be useful for rapid calculations in a real-time retrieval of the NET_{SFC} from NET_{TOA} or for the handling of large data volumes. It is suggested to fit detailed radiation calculations for a sufficient variety of climatological conditions with the proposed parameterization and then use the fits in the actual retrieval. Regression coefficients for the parameterization are provided for different conditions; however, updated regression coefficients should be recomputed on the basis of radiative transfer models that have been validated and modified, if necessary, through carefully designed high-resolution spectral measurements.

Major uncertainties in computed clear-sky solar absorption rates will remain due to the lack of information on aerosol, especially the absorbing component. In a direct retrieval of the solar surface net flux from the net at the top of the atmosphere, a bias in S_{ABS} will fully propagate into a bias in NET_{SFC}. Therefore, ancillary information on aerosol properties, either measured (Rao et al. 1989) or from climatology (d'Almeida et al. 1991), will significantly help in deriving an accurate global climatology of the net solar surface radiation from satellite-inferred net fluxes at the top of the atmosphere.

Acknowledgments. I thank Brian Mason and Leo van de Berg for reading the manuscript and offering helpful remarks. Thanks are due to the anonymous reviewers for constructive comments.

REFERENCES

Cess, R. D., and I. L. Vulis, 1989: Inferring surface albedo solar absorption from broadband satellite measurements. *J. Climate,* **2,** 974–985.

——, E. G. Dutton, J. J. DeLuisi, and F. Jiang, 1991: Determining surface solar absorption from broadband satellite measurements for clear skies: Comparison with surface measurements. *J. Climate,* **4,** 236–247.

——, S. Nemesure, E. G. Dutton, J. J. DeLuisi, G. L. Potter, and J. J. Morcrette, 1993: The impact of clouds on the shortwave radiation budget of the surface-atmosphere system: Interfacing measurements and models. *J. Climate,* **6,** 308–316.

Chertock, B., R. Frouin, and R. C. J. Somerville, 1991: Global monitoring of net solar irradiance at the ocean surface: Climatological variability and the 1982–1983 El Niño. *J. Climate,* **4,** 639–650.

Chou, M.-D., 1986: Atmospheric solar heating rate in the water vapor bands. *J. Appl. Meteor.*, **25,** 1532–1542.

——, 1989: On the estimation of surface radiation using satellite data. *Theor. Appl. Clim.*, **40,** 25–36.

——, 1990: Parameterizations for the absorption of solar radiation by O_2 and CO_2 with application to climate studies. *J. Climate,* **3,** 209–217.

——, 1991: The derivation of cloud parameters from satellite-measured radiances for use in surface radiation calculations. *J. Atmos. Sci.*, **48,** 1549–1559.

d'Almeida, G. A., P. Koepke, and E. P. Shettle, 1991: Atmospheric aerosols. Global climatology and radiative characteristics. A. Deepak, 561 pp.

Davies, R., W. L. Ridgway, and K. E. Kim, 1984: Spectral absorption of solar radiation in cloudy atmospheres: A 20 cm^{-1} model. *J. Atmos. Sci.*, **41,** 2126–2137.

Fischer, J., and H. Grassl, 1991: Detection of cloud-top height from backscattered radiances within the oxygen A band. Part 1: Theoretical study. *J. Appl. Meteor.*, **30,** 1245–1259.

Fouquart, Y., B. Bonnel, and V. Ramaswamy, 1991: Intercomparing shortwave radiation codes for climate studies. *J. Geophys. Res.*, **96**(D5), 8955–8968.

Grassl, H., 1975: Albedo reduction and radiative heating of clouds by absorbing aerosols. *Contrib. Atmos. Phys.*, **48,** 199–210.

Kasten, F., and A. T. Young, 1989: Revised optical air mass tables and approximation formula. *Appl. Opt.*, **28,** 4735–4738.

Kerschgens, M., U. Reuter, and E. Raschke, 1976: The absorption of solar radiation in model atmospheres. *Contrib. Atmos. Phys.*, **49,** 81–97.

Kiehl, J. T., C. Bruehl, and T. Yamanouchi, 1985: A parameterization for absorption due to the near infrared bands of CO_2. *Tellus,* **37B,** 189–196.

Kneizys, F. X., E. P. Shettle, W. O. Gallery, J. H. Chetwynd, L. W. Abreu, J. E. A. Selby, S. A. Clough, and R. A. Fenn, 1980: Atmospheric transmittance/radiance: Computer code LOWTRAN 5, AFGL-TR-80-0067, AD A058643, Air Force Geophysics Laboratory, Hanscom AFB, MA 01731.

Lacis, A. A., and J. E. Hansen, 1974: A parameterization for the absorption of solar radiation in the Earth's atmosphere. *J. Atmos. Sci.*, **31,** 118–133.

McClatchey, R. A., R. A. Fenn, J. E. A. Selby, F. E. Volz, and J. S. Garing, 1972: Optical properties of the atmosphere. 3rd ed., 110 p., Environm. Res. Pap. 411, Air Force Cambridge Res. Lab., Bedford, MA 02173.

McKee, T. B., and S. K. Cox, 1974: Scattering of visible radiation by finite clouds. *J. Atmos. Sci.*, **31,** 1885–1892.

Newiger, M., and K. Baehnke, 1981: Influence of cloud composition and geometry on the absorption of solar radiation. *Contrib. Atmos. Phys.*, **54,** 370–382.

Pinker, R. T., and J. D. Tarpley, 1988: The relationship between the planetary and surface net radiation: An update. *J. Appl. Meteor.*, **27,** 957–964.

Ramanathan, V., 1986: Scientific use of surface radiation budget data for climate studies. In: Surface radiation budget for climate applications. J. T. Suttles and G. Ohring, Eds., NASA Ref. Publ. 1169. NASA Washington, D.C. 20546-0001.

Ramaswamy, V., and S. M. Freidenreich, 1991: Solar radiative line-by-line determination of water vapor absorption and water cloud extinction in inhomogeneous atmospheres. *J. Geophys. Res.*, **96**(D5), 9133–9157.

Rao, C. N., L. L. Stowe, and E. P. McClain, 1989: Remote sensing of aerosols over the ocean using AVHRR data. Theory, practice and applications. *Int. J. Remote Sens.*, **10,** 743–749.

Raschke, E., and U. Stucke, 1973: Approximations of band transmission functions by finite sums of exponentials. *Contrib. Atmos. Phys.*, **46,** 203–212.

Rawlins, F., 1988: Aircraft measurements of the solar absorption of broken cloud fields: A case study. *Quart. J. Roy. Meteor. Soc.*, **115,** 365–382.

Schmetz, J., 1984: On the parameterization of the radiative properties of broken clouds. *Tellus,* **36A,** 417–432.

——, 1989: Towards a surface radiation climatology: Retrieval of downward irradiances from satellites. *Atmos. Res.*, **23,** 287–321.

——, 1991: Retrieval of surface radiation fluxes from satellite data. *Dyn. Atmos. Oceans,* **16,** 61–72.

——, and E. Raschke, 1978: A method to parameterize the solar radiation at ground. *Arch. Meteor. Geophys. Bioklim., Ser. B,* **26,** 143–151.

Stephens, G. L., 1979: Optical properties of eight water clouds. CSIRO Division of Atmospheric Physics. Technical Paper No. 36, 35 pp. [Available from Commonwealth Scientific and Industrial Research Organization, Station Street, Aspendale, Vic. 3195, Australia.]

Suttles, J. T., and G. Ohring, 1986: Surface radiation budget for climate applications. NASA Ref. Publ. 1169, NASA Washington, D.C., 20546-0001. 132 pp.

Wiscombe, W., and J. Evans, 1977: Exponential-sum fitting of radiative transmission functions. *J. Comput. Phys.*, **24,** 416–444.

——, R. M. Welch, and W. D. Hall, 1984: The effects of very large drops on cloud absorption. Part 1: Parcel models. *J. Atmos. Sci.*, **41,** 1336–1355.

World Climate Research Programme, 1986: A preliminary cloudless standard atmosphere for radiation calculations. Rep. WCP-112, 53 pp., World Meteor. Organ., Geneva.